Turkish Journal of Electrical Engineering & Computer Sciences

http://journals.tubitak.gov.tr/elektrik/

Research Article

Turk J Elec Eng & Comp Sci
(2016) 24: 3741 – 3758

doi:10.3906/elk-1410-127

A new market-based approach for daily Volt/Var control of distribution systems in the presence of distributed energy resources using Benders decomposition algorithm

Abouzar SAMIMI*, Ahad KAZEMI
Department of Electrical Engineering, Iran University of Science and Technology, Tehran, Iran

Received: 22.10.2014 • **Accepted/Published Online:** 11.06.2015 • **Final Version:** 20.06.2016

Abstract: Distributed energy resources (DERs), if properly coordinated with other Volt/Var control (VVC) devices, could be incorporated in daily VVC problem. In this paper, a new 2-stage model is presented for daily VVC of distribution systems including DERs, taking into account environmental and economic aspects. First, in the day-ahead market, an initial environmental-economic dispatch is performed to minimize both the electrical energy costs and the gas emissions pertaining to generation units. The initial scheduling results determined by the market operator are delivered to the second stage, namely the daily optimal dispatches of VVC devices, to examine them from operational viewpoints and to yield the daily optimal dispatches of the VVC devices. The objective function of the second stage consists of the total cost of the following components: active power losses, adjustment of the initially scheduled active powers, and depreciation of switchable devices. In this paper, attention is directed towards 2 important types of DERs to be connected to the network: synchronous machine-based distributed generations and wind turbines. Because the active and reactive powers of DERs are coupled via the capability diagram, in this paper, this issue is addressed by considering the capability diagram of DERs in the proposed model. In particular, the Q-capability diagram of wind turbines should be analyzed taking the hourly wind speed fluctuations into consideration, so that delivery of a uniform reactive power can be ensured over the entire hour of operation. Due to the complexity of solving mixed integer nonlinear programming problems, an algorithm based on Benders decomposition is suggested to solve the proposed VVC model in the second stage. Finally, 2 standard distribution test networks are utilized to validate the effectiveness of the proposed method.

Key words: Daily Volt/Var control, distributed energy resource, reactive power capability, wind turbine, adjustment bid, Benders' decomposition

1. Introduction

The main goal of conventional Volt/Var control (VVC) problem in distribution systems is the appropriate coordination between the on-load tap changer (OLTC) and all of the switched shunt capacitors (Sh.Cs) in order to achieve an optimum voltage profile over the distribution feeders and optimum reactive power flows in the system [1–4]. In recent years, due to environmental and economic considerations, distributed generations (DGs) have gained great interest. At present, most of the installed DGs are commonly operated at unity power factor in order to prevent interference with the conventional VVC devices of the distribution system [5]. However, the inverter embedded in DGs can provide reactive power based on a request from the distribution system operator

*Correspondence: abouzarsamimi@iust.ac.ir

(DSO). In [6], Viawan et al. investigated the effect of synchronous machine-based DGs on the available VVC and they also proposed a proper coordination strategy between DGs and other VVC devices.

Research on VVC in distribution systems can be categorized into 2 main frameworks: centralized control and decentralized control. Research on centralized control intends to determine dispatch schedules of all switched Sh.Cs, OLTC settings, and reactive power outputs of DGs for the next day based on the day-ahead load forecast [7–13]. In [7], a fuzzy adaptive particle swarm optimization methodology was proposed to solve the price-based compensation methodology for the daily VVC problem in distribution systems with dispatchable DG units. In [8], an analytic hierarchy process strategy and binary ant colony optimization algorithm were utilized to solve the multiobjective daily VVC of distribution systems. Oshiro et al. [9] proposed a combined genetic algorithm and tabu search (TS) approach for optimal voltage control taking into consideration the coordination of DGs, the load ratio control transformers, step voltage regulators, Sh.Cs, shunt reactors, and static Var compensators. In [10], a dynamic programming algorithm was used to solve the VVC problem, in which the DG output voltage was dispatched cooperatively with the operation of the OLTC and the Sh.Cs. Currently, wind turbines (WTs) are attracting attention from distribution companies (Discos) as the most common renewable energy sources (RESs). The stochastic nature of the wind speed poses an obstacle for operational planning of the distribution systems. Thus, probabilistic approaches are required to accommodate all uncertainties caused by wind power generation [11]. In [12], Liang et al. presented a fuzzy optimization approach to solve the VVC problem in a distribution system considering uncertainties in hourly load demands and wind speed forecast. In [13], an improved shuffled frog leaping algorithm was adopted to solve the multiobjective probabilistic VVC problem in distribution systems including wind farms and fuel cell power plants.

On the other hand, research on decentralized control aims to control the VVC equipment based on real-time and decentralized measurements and experiences [14,15]. Generally, this method provides no coordination between control devices. Furthermore, it is very difficult for decentralized control to take into account the constraints of the maximum allowable daily operating times of switchable equipment.

In all previous studies, the reactive power capability (Q-capability) of DERs has not been incorporated in the daily VVC problem of distribution systems. Specifically, the WT capability curve needs to be amended considering maximum hourly deviation of wind active power from the forecasted value. Moreover, the day-ahead active power market and the results of this market should be reflected in the daily VVC issue. These deficiencies motivated us to develop a new 2-stage model to achieve an economic/technical plan for the VVC problem of distribution systems in the presence of DERs. First, in the day-ahead market, a new environmental-economic dispatch problem is formulated to minimize the electrical energy costs and the gas emissions related to generation units. The results of the day-ahead market clearing are conveyed to the second stage, which is performed by the DSO, to check the feasibility of this schedule from operational viewpoints and to determine the daily optimal dispatch schedules for VVC devices. In this paper, 2 important types of DERs are considered to connect to the network: synchronous machine-based DGs and WTs. Due to the presence of integer and continuous control variables, the daily VVC of a distribution system has been considered as a mixed integer nonlinear programming (MINLP) problem. The complexity of solving MINLP optimization problems forced us to implement decomposition techniques, such as Benders decomposition algorithm. This specific technique of Benders decomposition algorithm had not been previously utilized in daily VVC problem. The proposed method, based on Benders decomposition, was applied to the 22-bus and IEEE 33-bus distribution systems and its performance was compared with the results obtained by a discrete and continuous optimizer program (DICOPT). The innovative contributions of this paper are as follows: 1) the Q-capability of DERs is considered

in the daily VVC problem, 2) the effect of day-ahead wind power forecast errors on Q-capability of WTs is considered in the daily VVC, 3) a comprehensive price-based model including depreciation cost of the switchable facilities is developed for the daily VVC problem, and 4) Benders decomposition algorithm is employed to solve the daily VVC problem.

2. Reactive power capability of DERs

2.1. Synchronous machine-based DG

Figure 1 depicts the capability curve of a synchronous machine-based DG (which will be simply called DG). For a scheduled active power (P_A), if the DG operates on the limiting curve (e.g., point A in Figure 1), any increase in reactive power provision by the DG will necessitate a reduction in the active power generation (point B in Figure 1). Hence, the DG is expected to receive a lost opportunity cost (LOC) payment for providing reactive power beyond Q_A [16]. In this paper, an adjustment bid [17] is utilized for opportunity cost payment. The adjustment bid is employed by a generation unit to indicate information about the price that the unit wants to receive for the reduction in its initial active power scheduled by the MO, together with the maximum change in its planned active power that it accepts. The adjustment bids of generation units are sent to the DSO. If the corresponding change in the scheduled active power has a negative value, represented by the ΔP^{Adj} variable, the opportunity cost payment can be calculated based on multiplying $\left|\Delta P^{Adj}\right|$ by the corresponding adjustment price (ρ_{Adj}). On the other hand, changes in the initial generation schedule of the DGs may be due to the enforcement of operation or security constraints. These changes can take both positive and negative values, which in both cases are compensated for by the adjustment prices.

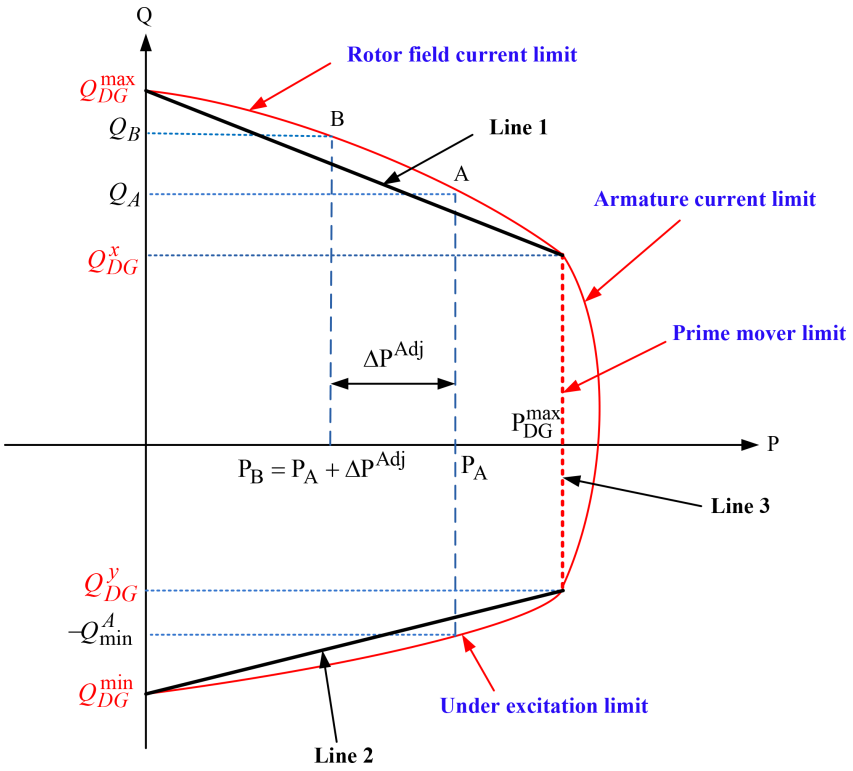

Figure 1. Capability diagram of a synchronous generator.

In order to model the capability diagram of a DG, the corresponding curves in the capability diagram can be approximated by linear expressions as follows:

- Line 1, between $(0, Q_{DG}^{\max})$ and $(P_{DG}^{\max}, Q_{DG}^{x})$, represents the rotor field current limit.
- Line 2, between $(0, Q_{DG}^{\min})$ and $(P_{DG}^{\max}, Q_{DG}^{y})$, represents the under excitation limit.
- Line 3, which is a vertical line, represents the prime mover limit of the turbine.

From a mathematical viewpoint, the constraint of the reactive power provision of a DG is given as:

$$Q_{DG}^{\min} + \frac{Q_{DG}^{y} - Q_{DG}^{\min}}{P_{DG}^{\max}}(P_A + \Delta P^{Adj}) \leq Q_{DG} \leq Q_{DG}^{\max} - \frac{Q_{DG}^{\max} - Q_{DG}^{x}}{P_{DG}^{\max}}(P_A + \Delta P^{Adj}) \tag{1}$$

It is worth mentioning that in Eq. (1), when the reactive power of a DG is greater than Q^A, the ΔP^{Adj} variable is activated, and otherwise it will be zero.

2.2. Wind turbine

In recent years, due to the development in wind speed forecasting techniques, the WT can be considered as a dispatchable energy resource by power system operators [18]. In [19], the capability curve of a WT with a full power back to back converter was extensively discussed. The active power generation of a WT is a function of wind speed as given in [20]. The converter's maximum voltage and current impose constraints on the reactive power capability of a WT. The maximum reactive power provision capability of a WT is given as [19]:

$$Q_{WT} = min\left\{Q_c, Q_v\right\} \tag{2}$$

$$Q_c = \sqrt{\left(V_g I_{c,\max}\right)^2 - P_{WT}^2} \tag{3}$$

$$Q_v = \sqrt{\left(\frac{V_g V_{c,\max}}{X}\right)^2 - P_{WT}^2} - \frac{V_g^2}{X} \tag{4}$$

Here, X represents the total reactance of the WT transformer, the grid filters, and the reactance of the transformer, which adapts the WT voltage to the grid voltage. Owing to the fluctuations of actual wind power from the forecasted value, delivery of the reactive power Q_{WT}, based on the forecasted active power P_{WT}^h, cannot be uniformly ensured by the WT over the entire hour of operation in the next day. Assuming that the maximum hourly variation of wind active power from the forecasted value ($\Delta P_{\max}$) is estimated using previous meteorological data, the available reactive power of the WT at the hth hour ($Q_{WT}^{h,av}$) can be determined as follows [19]:

$$Q_{WT}^{h,av} = \min\left\{Q_c^{h,av}, Q_v^{h,av}\right\} \tag{5}$$

where:

$$Q_c^{h,av} = \sqrt{\left(V_g I_{c,\max}\right)^2 - \left(P_{WT}^{h,\max}\right)^2} \tag{6}$$

$$Q_v^{h,av} = \sqrt{\left(\frac{V_g V_{c,\max}}{X}\right)^2 - \left(P_{WT}^{h,\max}\right)^2} - \frac{V_g^2}{X} \tag{7}$$

$$P_{WT}^{h,\max} = \min\left\{\left(P_{WT}^{h} + \Delta P_{\max}\right), P_{WT}^{rated}\right\} \tag{8}$$

The available reactive power capability of a wind generator is illustrated in Figure 2. If the WT is requested by the DSO to produce $Q_{WT}^{h,req}$ that is more than $Q_{WT}^{h,av}$, then its active power generation is restricted to $P_{WT}^{h,lim}$. Thus, the WT may forgo selling active power $\left|\Delta P_{WT}^{chg,h}\right|$ in the energy market or energy balance service market, where:

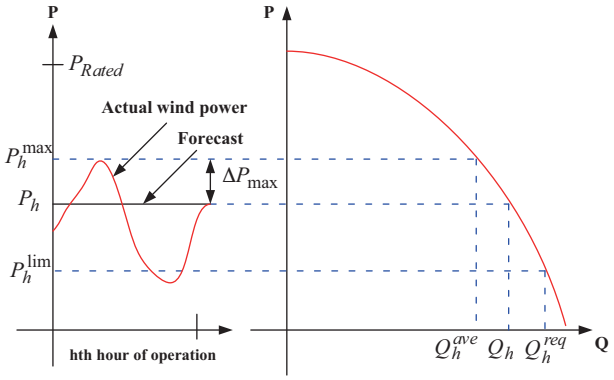

Figure 2. Reactive power capability of a wind turbine considering the hourly wind power fluctuations.

$$\Delta P_{WT}^{chg,h} = P_{WT}^{h,lim} - P_{WT}^{h,max} \tag{9}$$

Accordingly, the LOC is calculated using the adjustment price offered by the WT as follows:

$$LOC_{WT} = \begin{cases} k\left(P_{WT}^{h,max} - P_{WT}^{h,lim}\right)\rho_{Adj} & P_{WT}^{h,lim} \geq P_{WT}^{h} \\ k\left(P_{WT}^{h,max} - P_{WT}^{h}\right)\rho_{Adj} + \rho_{Adj} & P_{WT}^{h,lim} < P_{WT}^{h} \end{cases} \tag{10}$$

where $0 < k < 1$. Since WT active power production may need to be decreased only for a fraction of an hour, in accordance with coefficient k, to provide the requested reactive power, the calculation of LOC based on $P_{WT}^{h,max}$ may give rise to overcompensation for the WT.

3. Initial environmental-economic dispatch problem

The initial environmental-economic dispatch (IEED) represents a multiobjective optimization problem to minimize the gas emissions and the electrical energy costs of generation units. For this purpose, in the day-ahead market, the generation units offer selling bids that consist of couples quantity and price to the MO. Hence, the total costs of electrical energy generated by the Disco and the DERs are calculated as:

$$COST_{Energy} = \sum_{h=1}^{Nh} P_{Disco}^{h} \times \pi_{Disco}^{h} + \sum_{h=1}^{Nh}\sum_{i=1}^{NDER} P_{DER,i}^{h} \times \pi_{DER,i}^{h} \tag{11}$$

The most important emissions from the electricity sector are SO_2, NO_x, and CO_2, which are represented by the sum of a quadratic and exponential function of the generated power for SO_2 and NO_x and released pollution in terms of tons per MW for the CO_2 [21,22]. In order to economically illustrate the harmful effects of the emissions on the environment, different techniques, such as penalties through carbon taxes or a cap-and-trade technique, have been utilized [22]. In this study, based on the penalties through the carbon taxes technique, penalty cost functions of the CO_2 emissions pertaining to the Disco and the DERs are calculated as follows:

$$COST_{Disco}^{Emissions} = \sum_{h=1}^{Nh} P_{Disco}^{h} \left(CO_{2,Disco} - CO_{2,cap}\right) EPC_{CO2} \tag{12}$$

$$COST_{DER}^{Emissions} = \sum_{h=1}^{Nh} \sum_{i=1}^{NDER} P_{DER,i}^{h} \left(CO_{2,DER,i} - CO_{2,cap}\right) EPC_{CO2} \tag{13}$$

Consequently, the total penalty cost of CO_2 emissions originating from generation units is expressed as:

$$COST_{Emissions} = COST_{Disco}^{Emissions} + COST_{DER}^{Emissions} \tag{14}$$

The MO runs the IEED problem, which can be modeled by Eqs. (15)–(18), as a uniform price auction for the entire distribution system and determines the accepted selling bids and hourly initial dispatch for the next day. Moreover, the maximum selling bid price accepted for each hour denotes the hourly market clearing price (MCP).

- *Objective function:*

$$\min Z = COST_{Energy} + COST_{Emissions} \tag{15}$$

Constraints:

$$0 \le P_{Disco}^{h} \le PBid_{Disco}^{h} \tag{16}$$

$$0 \le P_{DER,i}^{h} \le PBid_{DER,i}^{h} \tag{17}$$

$$P_{Disco}^{h} + \sum_{i=1}^{NDER} P_{DER,i}^{h} = \sum_{i=1}^{Nbus} P_{D,i}^{h} \tag{18}$$

Eqs. (16) and (17) represent the limits on the generations and Eq. (18) represents the constraint of demand/supply balance. The results of the initial schedule prepared by the MO are submitted to the DSO to verify them from operational viewpoints. If the technical infeasibilities of operation or violations of security constraints occur, the DSO activates the adjustment bids of generation units to modify the initial schedule.

4. Proposed formulation for daily optimal dispatches of VVC devices

In order to achieve the daily optimal dispatches of VVC devices all generation units should first submit their adjustment bids to the DSO. Moreover, the results of IEED obtained by the MO are sent to the DSO. Then the DSO performs the VVC using an optimization problem as follows.

4.1. Objective function

The proposed objective function of the daily VVC problem consists of 3 components as follows:

- Cost of total active power losses:

In order to balance the total active power losses in the distribution system, the nonnegative variables of ΔP^{L}_{DER} and ΔP^{L}_{Disco} corresponding to the increase of the initially scheduled active power are allocated to each DER and Disco, respectively. The cost of total active power losses is achieved multiplying these variables by the MCP as in Eq. (19):

$$f_1 = \sum_{h=1}^{Nh} \Delta P^{L,h}_{Disco} \times MCP^h + \sum_{h=1}^{Nh} \sum_{i=1}^{NDER} \Delta P^{L,h}_{DER,i} \times MCP^h \tag{19}$$

- Cost of adjustment of IEED:

Adjustment of the initially scheduled active power of generation units (i.e. IEED) may be required due to the enforcement of operation constraints or to enable a certain level of reactive power provision. The cost of adjustment of the IEED is calculated based on the values of generation adjustments and the respective adjustment prices as follows:

$$f_2 = \sum_{h=1}^{Nh} \left|\Delta P^{Adj,h}_{Disco}\right| \times \rho^{h}_{Adj\,Disco} + \sum_{h=1}^{Nh} \sum_{i=1}^{NDG} \left|\Delta P^{Adj,h}_{DG,i}\right| \times \rho^{h}_{Adj\,DG,i} + \sum_{h=1}^{Nh} \sum_{i=1}^{NWT} LOC^{h}_{WT,i} \tag{20}$$

- Costs of switching operations of OLTC and switched Sh.Cs:

Switchable devices like OLTC and Sh.Cs are permitted to be operated for a limited number of switching operations during their entire lifetime. Thus, depreciation in the capital cost originating from each switching operation is represented in terms of $/switching operation [23]. Costs of the switching operations of the OLTC and switched Sh.Cs over the entire scheduling horizon are expressed as in Eq. (21):

$$f_3 = \sum_{h=1}^{Nh-1} D_{Tap} \left|Tap^{h+1} - Tap^{h}\right| + \sum_{h=1}^{Nh-1} \sum_{i=1}^{NSC} D_S \left|CStep^{h+1}_{i} - CStep^{h}_{i}\right| \tag{21}$$

Finally, the objective function of the daily VVC problem can be expressed as follows:

$$\min f = f_1 + f_2 + f_3 \tag{22}$$

4.2. Constraints

The objective function of VVC is minimized subject to power balancing equality constraints as well as the following inequality constraints:

- Bus voltage magnitude:

$$V_{\min} \le \left|V^{h}_{i}\right| \le V_{\max} \tag{23}$$

- Limits of the active power adjustments of Disco and DERs:

$$-x^{\max}_{Disco} \times P^{ini,h}_{Disco} \le \Delta P^{Adj,h}_{Disco} \le x^{\max}_{Disco} \times P^{ini,h}_{Disco} \tag{24}$$

$$-x^{\max}_{DER,i} \times P^{ini,h}_{DER,i} \leq \Delta P^{Adj,h}_{DER,i} \leq x^{\max}_{DER,i} \times P^{ini,h}_{DER,i} \tag{25}$$

- Limits of generation capacity:

$$P^{\min}_{Disco} \leq P^{ini,h}_{Disco} + \Delta P^{L,h}_{Disco} + \Delta P^{Adj,h}_{Disco} \leq P^{\max}_{Disco} \tag{26}$$

$$P^{\min}_{DER,i} \leq P^{ini,h}_{DER,i} + \Delta P^{L,h}_{DER,i} + \Delta P^{Adj,h}_{DER,i} \leq P^{\max}_{DER,i} \tag{27}$$

- Limit of reactive power generation of Disco:

$$Q^{h,min}_{Disco} \leq Q^{h}_{Disco} \leq Q^{h,max}_{Disco} \tag{28}$$

- Limit of transformers tap:

$$Tap_{\min} \leq Tap^{h} \leq Tap_{\max} \tag{29}$$

- Limit of steps of capacitors:

$$CStep^{\min}_{i} \leq CStep^{h}_{i} \leq CStep^{\max}_{i} \tag{30}$$

- Maximum permissible daily number of OLTC operations:

$$\sum_{h=1}^{Nh-1} \left| Tap^{h+1} - Tap^{h} \right| \leq N^{\max}_{OLTC} \tag{31}$$

- Maximum permissible daily number of switching operations of Sh.Cs:

$$\sum_{h=1}^{Nh-1} \left| CStep^{h+1}_{i} - CStep^{h}_{i} \right| \leq N^{\max}_{Sh.C,i} \tag{32}$$

5. Solution methodology based on Benders decomposition algorithm

The proposed daily VVC model is formulated as a MINLP problem. The complexity of solving MINLP problems forces us to implement decomposition techniques, such as Benders decomposition algorithm. The general MINLP problem is decomposed by means of Benders decomposition algorithm into 2 structures, master and slave. The proposed solution methodology is programmed in GAMS software using the CPLEX solver for solving the mixed integer programming (MIP) of the master problem and the CONOPT solver for solving the nonlinear programming (NLP) of the slave problem. Benders decomposition algorithm is described as follows:

Master problem: The master problem decides the tap setting of the OLTC and the steps of Sh.Cs in order to minimize the costs of switching operations. Therefore, all integer variables should be included in the optimization of the master problem. The objective function of the master problem minimizes as:

$$f_{master} = f_3 + \alpha \tag{33}$$

subject to the constraints of Eqs. (29)–(32) and the following Benders linear cuts:

$$\alpha \geq f_{slave}^{(m)} + \sum_{h=1}^{Nh} \sum_{i=1}^{NSC} \lambda_i^{h(m)} \left(CStep_i^h - CStep_i^{h(m)} \right) + \sum_{h=1}^{Nh} \mu^{h(m)} \left(Tap^h - Tap^{h(m)} \right) m = 1, 2, \ldots, v-1 \quad (34)$$

The only real variable α in Eqs. (33) and (34) is an underestimation of the slave problem costs, which contain the infeasibility costs. Benders linear cuts, which are updated every iteration, join the master and slave problems. An additional cut is added to the master problem in every iteration.

Slave problem: The slave problem formulation is very similar to the main problem, in that all integer variables are fixed to given values determined by the master problem. However, in some cases, the master problem solution makes an infeasible NLP slave problem. To avoid these cases, at each iteration, the artificial variables are added to some constraints and are embedded in the objective function so that the objective function minimizes the technical infeasibilities of operation. Moreover, the slave problem gives the optimal dispatches of generation units. The slave problem is formulated as below:

$$f_{slave} = f_1 + f_2 + M \sum_{h=1}^{Nh} \sum_{i \in L} \left(u_i^h + w \right) \quad (35)$$

It is subject to the constraints of Eqs. (23)–(28), active power balancing equations, and the following constraints:

$$\left(Q_{G,i}^h + q_i^h \right) - Q_{D,i}^h = \left| V_i^h \right| \sum_{j=1}^{NBus} \left| V_j^h \right| |Y_{ij}| \sin \left(\theta_i^h - \theta_j^h - \varphi_{ij} \right) \quad (36)$$

$$q_i^h = \begin{cases} u_i^h - w & i \in L \\ 0 & otherwise \end{cases} \quad (37)$$

$$CStep_i^h = CStep_i^{h(v-1)} : \lambda_i^{h(v)} \quad Tap^h = Tap^{h(v-1)} : \mu^{h(v)} \quad (38)$$

Here, u_i^h and w are the positive artificial variables of the optimization problem and M is a large enough positive constant. Eq. (38) demonstrates the dual variables (sensitivities) associated with the discrete variables specified previously by the master problem.

Stopping criterion:

Benders decomposition algorithm ends when, in the first place, the solution created by the master problem is feasible, and, secondly, when the slave problem costs computed through the slave problem (upper bound) and the variable α (lower bound) computed through the master problem are close enough. The procedure of Benders decomposition algorithm for the proposed 2-stage model of daily VVC is shown in Figure 3.

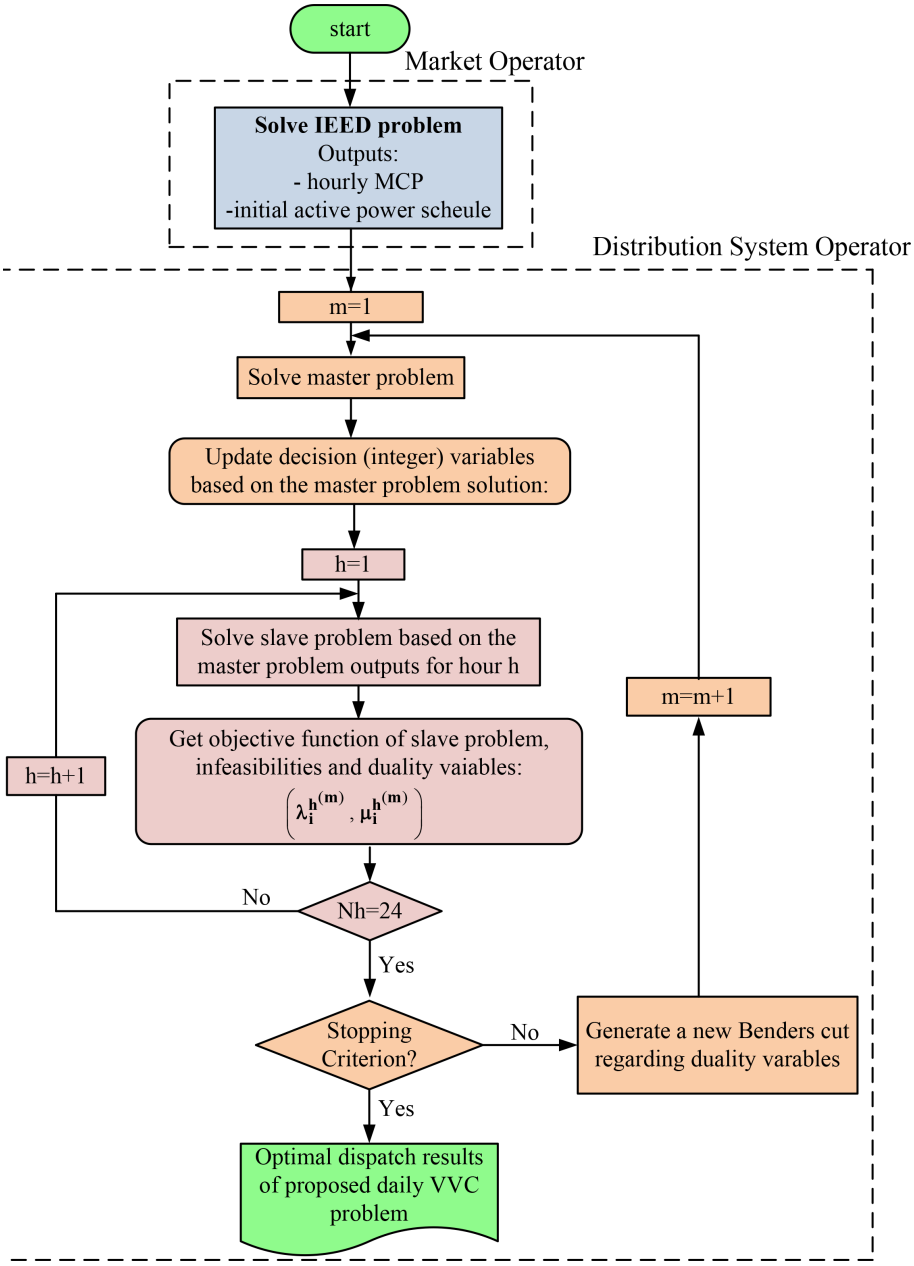

Figure 3. Flowchart of the optimization problem based on Benders decomposition algorithm.

6. Simulation results

In this section the proposed method for the daily VVC is examined on 2 distribution systems.

6.1. The 22-bus distribution system

The 22-bus 20-kV radial distribution test system [14] is modified and used in this study. The single-line diagram of the test distribution network is shown in Figure 4. The HV/MV tap changing transformer has 11 tap positions and each tap ratio is 0.01 p.u. Voltage limits are considered as $\pm$ 5% of nominal voltage. The capacitor banks C1 and C2 have the capacity of 1000 kVAr with 5 switching steps of 200 kVAr. Three DERs including 2 DGs

and 1 WT are connected to the distribution system. The data of the DERs are listed in Table 1. The values of $CO_{2,cap}$ and EPC_{CO2} are assumed as 0.1 t/MWh and 40 $/t, respectively [24]. The maximum hourly variation of the actual wind power from the forecasted value is considered as 10% of the forecasted value.

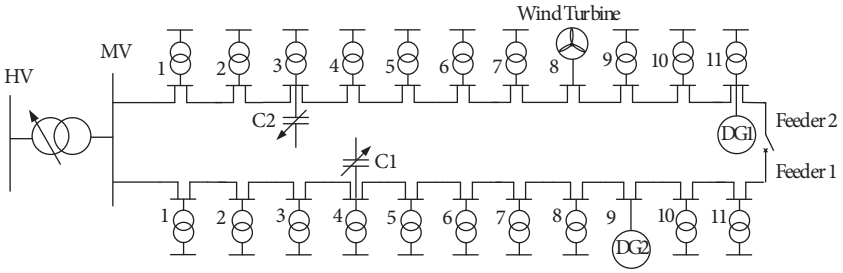

Figure 4. The single-line diagram of a 22-bus distribution test system.

Table 1. Characteristics of the distributed energy resources of the 22-bus distribution system.

	Capacity (kW)	CO_2 (t/MWh)	$P_{DG}^{\max}$ (kW)	$Q_{DG}^{\max}$ (kVAr)	$Q_{DG}^{\min}$ (kVAr)	Q_{DG}^{x} (kVAr)	Q_{DG}^{y} (kVAr)	ρ_{Adj}	$x^{\max}$
DG1	400	0.489	400	400	–400	200	–400	0.08	50%
DG2	1000	0.724	1000	1000	–600	600	–500	0.075	50%

	Capacity (kW)	CO_2 (t/MWh)	$V_{c,\max}$ (p.u.)	$I_{c,\max}$ (p.u.)	X (p.u.)	$Q_{WT}^{\min}$ (kVAr)	ρ_{Adj} ($/kWh)	$x^{\max}$
WT	500	0	1.4	1.24	0.2	–250	0.095	50%

6.1.1. IEED obtained by the MO

The linear programming problem of IEED is modeled in GAMS and solved by the CPLEX solver. This program provides the hourly MCP and the accepted bid power of each generation unit for the next day. Table 2 demonstrates the results of IEED of the generation units and hourly MCP.

Table 2. Initial environmental-economic schedule for the 22-bus distribution system.

Hour	P_{Disco}^{ini} (kW)	P_{DG1}^{ini} (kW)	P_{DG2}^{ini} (kW)	P_{WT}^{ini} (kW)	MCP ($/kWh)	Hour	P_{Disco}^{ini} (kW)	P_{DG1}^{ini} (kW)	P_{DG2}^{ini} (kW)	P_{WT}^{ini} (kW)	MCP ($/kWh)
1	422.6	300	400	100	0.05	13	4264.6	400	800	442	0.06
2	76.1	300	400	100	0.05	14	2056.3	400	1000	442	0.06
3	468.9	300	400	100	0.05	15	260.7	400	1000	442	0.06
4	626.4	300	400	100	0.05	16	187.9	400	1000	500	0.06
5	659.9	300	400	100	0.05	17	2008.1	400	1000	500	0.06
6	691.4	300	400	100	0.05	18	5069.8	400	1000	500	0.06
7	488.4	300	400	366	0.05	19	5897	400	1000	480	0.06
8	801.4	300	400	366	0.05	20	5756.2	400	1000	480	0.06
9	1375.4	400	800	366	0.06	21	4646.8	400	1000	480	0.06
10	4003.9	400	800	366	0.06	22	2925.0	400	1000	480	0.06
11	4651.5	400	800	442	0.06	23	598.9	400	800	100	0.06
12	4758.8	400	800	442	0.06	24	80.1	400	800	100	0.06

6.1.2. Daily optimal dispatches of VVC devices

The adjustment price offered by the Disco, the maximum admitted change in its initial scheduled active power, and CO_2 emissions related to its activities are 0.09 \$/kWh, 100%, and 0.927 t/MWh, respectively. The installation cost of the OLTC is assumed to be \$400,000 as reported in [23]. The total number of acceptable switching operations of each OLTC can be 143,080 times (= 20 steps/day ×365 days/year ×20 years ×0.98 availability factor). Thus, the depreciation cost for each step change (D_{Tap}) is \$2.79. The installation cost for each Sh.C is \$11,600 [23]. Each Sh.C can be operated 71,540 times (= 10 switching operations/day ×365 days/year ×20 years ×0.98 availability factor). Therefore, the depreciation cost for each switching operation of a Sh.C (D_S) is equal to \$0.162. The proposed VVC model will be tested on 3 different cases through the 22-bus distribution system as follows.

6.1.3. Case 1 - Base case and implementing Benders decomposition algorithm

By implementing Benders decomposition algorithm, Figure 5 depicts the hourly optimal dispatches of the Sh.Cs for the base case of the network. The number of switching operations for C1 and C2 is 6 and 8, respectively, which is less than the maximum allowable daily number of operations (10 times). Furthermore, the high depreciation cost of the OLTC causes the tap position of the OLTC to be fixed at 1.04 p.u. during the whole day. Table 3 gives the optimal dispatches of generation units concerning the changes in the IEED and reactive power provision. In this case, the change in the IEED corresponding to operation or security enforcements is not necessary and all constraints are well satisfied through the proposed optimization method, so all the ΔP^{Adj} variables are zero. Regarding the ΔP^{L} variables, these variables are zero for DG1 and WT for all hours. Hence, the power losses of the system are balanced in 2 buses using the Disco and DG2 during the next day. Moreover, after applying VVC, the voltages of buses are brought back to the acceptable range of 0.95 p.u. to 1.05 p.u. for all hours.

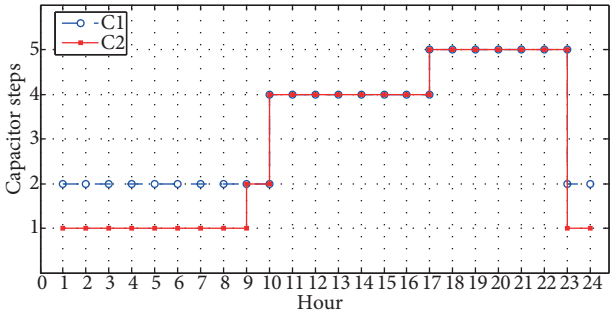

Figure 5. Daily optimal dispatches of the shunt capacitors for case 1.

6.1.4. Case 2 - Relaxing limits of the switching operations and implementing the DICOPT solver

In order to validate the results obtained by the proposed approach, the same problem has been tested by relaxing all constraints of the daily number of switching operations, while the costs of the switching operations in the objective function are disregarded. In this case, since the optimal dispatch results of OLTC and Sh.Cs for each hour are not correlated with the solutions of the other hours, the daily VVC problem can be separately solved for each hour via the DICOPT solver. For this case, the daily optimal dispatches of the OLTC and Sh.Cs are illustrated, respectively, in Figures 6 and 7. As seen in Figure 7, the number of operations of C1 and C2 is,

Table 3. Daily optimal dispatch of generation units for case 1 in the 22-bus distribution system.

Hour	Disco			DG1			DG2			WT		
	ΔP^L (kW)	ΔP^{Adj} (kW)	Q (kVAr)	ΔP^L (kW)	ΔP^{Adj} (kW)	Q (kVAr)	ΔP^L (kW)	ΔP^{Adj} (kW)	Q (kVAr)	ΔP^L (kW)	ΔP^{Adj} (kW)	Q (kVAr)
1	1.84	0	0	0	0	75.46	0	0	38.85	0	0	81.22
2	2.12	0	0	0	0	47.53	0	0	–66.49	0	0	0
3	1.84	0	0	0	0	79.64	0	0	54.91	0	0	95.68
4	1.88	0	39.18	0	0	87.95	0.29	0	83.78	0	0	117.23
5	0	0	51.14	0	0	86.23	2.39	0	83.86	0	0	115.79
6	0	0	59.96	0	0	87.89	2.50	0	89.18	0	0	119.60
7	0	0	76.91	0	0	91.22	3.45	0	99.84	0	0	128.56
8	0	0	162.04	0	0	111.22	4.10	0	158.43	0	0	171.48
9	0	0	318.26	0	0	190.84	8.26	0	379.60	0	0	262.15
10	0	0	999.94	0	0	200	59.95	0	656.02	0	0	471.50
11	0	0	1676.57	0	0	200	90.03	0	643.99	0	0	384.72
12	0	0	1768.54	0	0	200	95.73	0	641.71	0	0	384.72
13	0	0	1372.04	0	0	200	72.60	0	650.96	0	0	384.72
14	15.71	0	88.09	0	0	200	0	0	421.50	0	0	361.50
15	12.34	0	0	0	0	–59.82	0	0	–177.8	0	0	0
16	13.10	0	0	0	0	–67.32	0	0	–184.8	0	0	0
17	16.63	0	0	0	0	200	0	0	244.30	0	0	173.42
18	110.43	0	1782.07	0	0	200	0	0	600	0	0	366.61
19	160.52	0	2399.50	0	0	200	0	0	600	0	0	366.61
20	151.79	0	2298.42	0	0	200	0	0	600	0	0	366.61
21	92.48	0	1503.54	0	0	200	0	0	600	0	0	366.61
22	31.71	0	266.06	0	0	200	0	0	553.29	0	0	366.61
23	5.44	0	168.03	0	0	113.21	0	0	168.04	0	0	174.61
24	5.84	0	25.17	0	0	84.11	0	0	78.01	0	0	109.44

respectively, 13 and 18 times, which is higher than the maximum acceptable switching operations. In order to confirm the effectiveness of the proposed method based on Benders decomposition algorithm, Table 4 provides a comparison between the results of cases 1 and 2. From the comparison of results presented in Table 4, it can be observed that despite the limited switching operations that are considered in the Benders decomposition-based proposed model, the total cost decreases to \$59.842, compared to \$77.132 when no restriction is imposed on the switched devices. On the other hand, when the limitations on switching operations of control devices are not considered, the active power losses decrease from 962.96 kW to 926.14 kW. This is due to the fact that an unlimited number of switching operations provides a more flexible and gentler control of the power flow to regulate the voltage within its admissible range and to fulfill the operational constraints.

6.1.5. Case 3 - Stressed operation situation for peak hours and implementing Benders decomposition algorithm

In case 3, the proposed model is tested while admitting that due to the operational issues, the maximum reactive power of the Disco is limited for peak hours (hours 18–21) to get a more stressed operation situation. The maximum reactive power of the Disco is decreased by 1600 kVAr, 2200 kVAr, 2200 kVAr, and 1400 kVAr

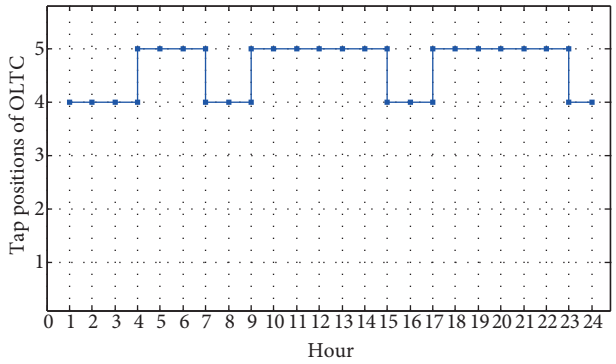

Figure 6. Daily optimal tap positions of on-load tap changer for case 2.

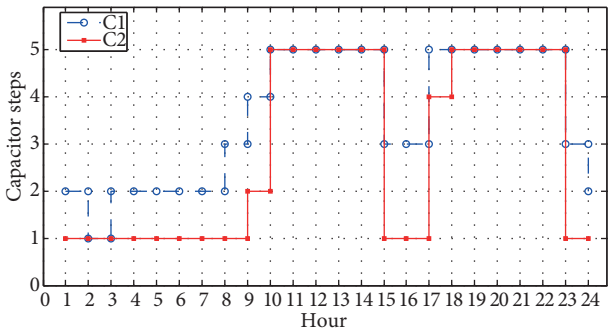

Figure 7. Daily optimal dispatches of the shunt capacitors for case 2.

Table 4. Comparison of optimization results in cases 1 and 2 for the 22-bus distribution system.

	Case 1	Case 2
Total active power losses (kWh)	962.96	926.14
Depreciation cost of OLTC ($)	0	16.74
Depreciation cost of Sh.Cs ($)	2.268	5.022
Total cost of active power losses ($)	57.574	55.37
Total cost ($)	59.842	77.132

at hours 18, 19, 20, and 21, respectively. Table 5 presents the results of reactive power dispatches of generation units for peak hours. As indicated in Table 5, the ΔP^{Adj} variable is not zero for the Disco, DG1, and DG2. The scheduled reactive powers of DG1 and DG2 are increased to fulfill the reduction of the reactive power of the Disco. Furthermore, a reduction in the active power generations of DG1 and DG2 takes place to adjust for the reactive power requirements of the system. It is worth mentioning that the other results of daily optimal dispatches of generation units, OLTC, and Sh.Cs are not changed. Concerning the objective function, its final value will be $294.86. This value is much greater than the one given in case 1 because it includes the adjustment costs of the initially scheduled active powers.

Table 5. Daily optimal reactive power dispatches of generation units for peak h for case 3.

Hour	Disco			DG1			DG2			WT		
	ΔP^{L} (kW)	ΔP^{Adj} (kW)	Q (kVAr)	ΔP^{L} (kW)	ΔP^{Adj} (kW)	Q (kVAr)	ΔP^{L} (kW)	ΔP^{Adj} (kW)	Q (kVAr)	ΔP^{L} (kW)	ΔP^{Adj} (kW)	Q (kVAr)
18	128.5	445.6	1600	0	–200	300	0	–245.6	698.2	0	0	366.6
19	184.8	503.2	2200	0	–200	300	0	–303.2	721.3	0	0	366.6
20	160.8	216.2	2200	0	–200	300	0	–16.2	606.5	0	0	366.6
21	100.7	227.2	1400	0	–200	300	0	–27.2	610.9	0	0	366.6

6.2. IEEE 33-bus distribution system

The IEEE 33-bus distribution system [8,24] is modified and considered as the second case study. Two DG units and a WT are assumed to be connected to the distribution system as illustrated in Figure 8. The capacity

of DERs connected to buses 18, 22, and 33 is 1000, 400, and 700 kW, respectively. The maximum hourly variation of the actual wind power from the forecasted value is considered as 20% of the forecasted value. The depreciation cost for each step change (D_{Tap}) of the OLTC is \$1.3. Moreover, the depreciation cost for each switching operation (D_S) of C1, C2, and C3 is considered as \$0.1, \$0.081, and \$0.081, respectively. The other conditions of this case study are considered as in the 22-bus distribution system.

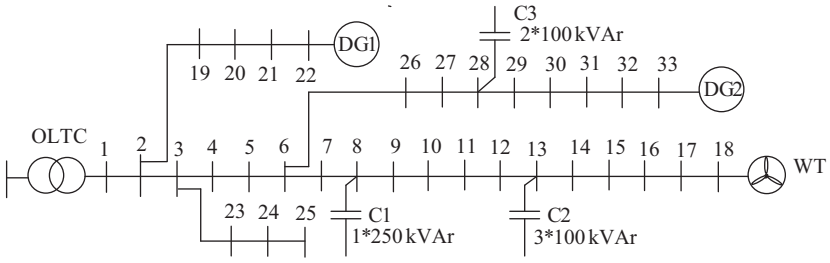

Figure 8. The single-line diagram of the IEEE 33-bus distribution test system.

By employing Benders decomposition algorithm, the optimal dispatch schedules of the OLTC and switched Sh.Cs are represented in Figures 9 and 10, respectively. The costs of the switching operations of the OLTC and switched Sh.Cs over the entire scheduling horizon are \$2.6 and \$0.686, respectively. As can be observed from Table 6, these values are considerably lower than the ones obtained when the costs of the switching operations and all constraints of the daily number of switching operations are disregarded. In this simulation, all the ΔP^{Adj} variables are zero. Furthermore, the total active power losses of the system are 2537.8 kW, from which 2295.4 kW is balanced by the Disco and 242.4 kW by DG2. The final scheduled active and reactive powers of generation units are depicted in Figures 11 and 12.

Table 6. Optimization results for 2 different cases in the IEEE 33-bus distribution system.

	Proposed method	Without switching operations
Total active power losses (kWh)	2537.805	2523.68
Depreciation cost of OLTC (\$)	2.6	7.8
Depreciation cost of Sh.Cs (\$)	0.686	1.172
Total cost of losses (\$)	149.519	148.716
Total cost (\$)	152.805	157.688

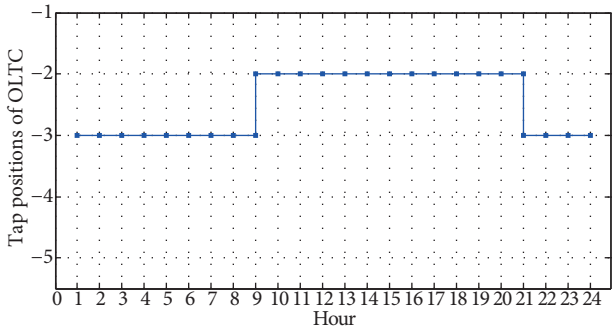

Figure 9. Daily optimal tap positions of on-load tap changer for the IEEE 33-bus distribution system.

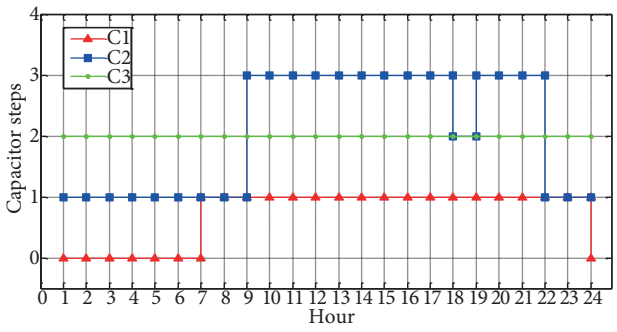

Figure 10. Daily optimal dispatches of the shunt capacitors for the IEEE 33-bus distribution system.

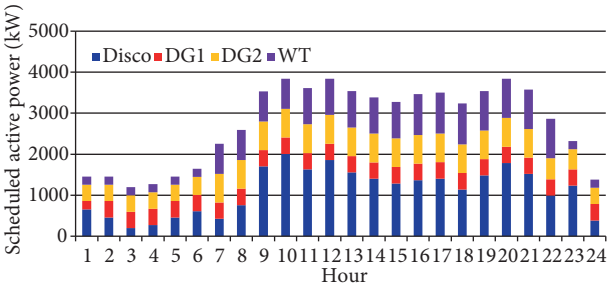

Figure 11. Final scheduled active power of generation units for the IEEE 33-bus distribution system.

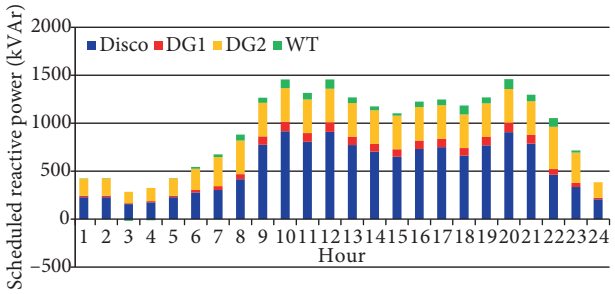

Figure 12. Scheduled reactive power of generation units for the IEEE 33-bus distribution system.

7. Conclusion

This paper presented a new approach based on the complete active/reactive power dispatch for the daily VVC in distribution networks. The proposed model was composed of 2 stages. In the first stage, the initial active power scheduling of generation units was determined by the MO in order to minimize the gas emissions and energy costs of generation units. The results of the first stage were conveyed to the second stage, which deals with daily optimal dispatches of VVC devices, to validate them from the technical viewpoints. Furthermore, in the second stage, the daily optimal dispatches of VVC devices were determined by the DSO. Due to the coupling between active and reactive power of DERs, the capability diagrams of DERs were incorporated in the proposed model. Benders decomposition technique was applied to cope with the complexity of solving the daily VVC problem as a MINLP problem. Two typical distribution systems were utilized to demonstrate the effectiveness of the proposed methodology. The simulation results revealed that the proposed VVC method is very efficient in attaining an optimal dispatching schedule in an economic manner and bringing the voltages of buses back to their acceptable limits.

Nomenclature

NDER / NDG / NWT / Nh	total number of the distributed energy resources / distributed generations / wind turbines / hours
L	set of buses that have switched capacitor
$P^h_{DER,i}/P^h_{Disco}$	generated active power by the ith distributed energy resource / distribution company at the hth hour
$\pi^h_{DER,i}/\pi^h_{Disco}$	price of the electrical energy offered by the ith distributed energy resources / distribution company at the hth hour
$CO_{2,Disco}/CO_{2,DER,i}$	CO_2 emissions pertaining to distribution company / ith distributed energy resources (t/MW)
$CO_{2,cap}$	permissible CO_2 emissions (t/MW)
EPC_{CO2}	CO_2 emissions penalty cost ($/t)
MCP^h	market clearing price at the hth hour
$PBid^h_{Disco}/PBid^h_{DER,i}$	maximum active power bid quantity offered by distribution company / ith distributed energy resource at the hth hour
$P^h_{D,i}$	active power of load demand at bus i at the hth hour
Tap^h	tap position of on-load tap changer at hth hour
$CStep^h_i$	step position of ith switched shunt capacitor at hth hour

D_{Tap}	depreciation cost for each step change of on-load tap changer
D_S	depreciation cost for each switching operation of shunt capacitor
$Tap_{min}(Tap_{\max})$	minimum (maximum) tap position of on-load tap changer
$CStep_i^{min}(CStep_i^{\max})$	minimum (maximum) step of ith shunt capacitor
$N_{OLTC}^{\max}/N_{Sh.C,i}^{\max}$	maximum permissible daily number of operations of on-load tap changer / ith shunt capacitor
$P_{Disco}^{ini,h}/P_{DER,i}^{ini,h}$	active power of distribution company / ith distributed energy resource scheduled by the MO at hth hour
$\Delta P_{Disco}^{L,h}/\Delta P_{DER,i}^{L,h}$	change in initial scheduled active power corresponding to the contribution of distribution company / ith distributed energy resource to balance active losses at hth hour
$P_{Disco}^{Adj,h}/P_{DER,i}^{Adj,h}$	amount of generation adjustment of distribution company / ith distributed energy resource at hth hour due to the enforcement of operation constraints
$x_{Disco}^{\max}/x_{DER,i}^{\max}$	maximum changes regarding the initial scheduled active power admitted by distribution company / ith distributed energy resource
$\rho_{Adj\,Disco}^{h}/\rho_{Adj\,DER,i}^{h}$	adjustment price offered by distribution company / ith distributed energy resource at hth hour
$Q_{Disco}^{h}/Q_{DER,i}^{h}$	reactive power provided by distribution company / ith distributed energy resource at hth hour
$I_{c,\max}(V_{c,\max})$	converter's maximum current (voltage) of wind turbine
λ_i^h/μ^h	dual variable of $CStep_i^h/Tap^h$

References

[1] Park JY, Nam SR, Park JK. Control of a ULTC considering the dispatch schedule of capacitors in a distribution system. IEEE T Power Syst 2007; 22: 755-761.

[2] Hu Z, Wang X, Chen H, Taylor GA. Volt/Var control in distribution systems using a time-interval based approach. IEE P Gener Transm Distrib 2003; 150: 548-554.

[3] Liang RH, Wang YS. Fuzzy-based reactive power and voltage control in a distribution system. IEEE T Power Deliver 2003; 18: 610-618.

[4] Liu MB, Canizares CA, Huang W. Reactive power and voltage control in distribution systems with limited switching operations. IEEE T Power Syst 2009; 24: 889-899.

[5] Al Abri RS, El-Saadany EF, Atwa YM. Optimal placement and sizing method to improve the voltage stability margin in a distribution system using distributed generation. IEEE T Power Syst 2013; 28: 326-334.

[6] Viawan F, Karlsson D. Voltage and reactive power control in systems with synchronous machine-based distributed generation. IEEE T Power Deliver 2008; 23: 1079-1087.

[7] Niknam T, Firouzi B, Ostadi A. A new fuzzy adaptive particle swarm optimization for daily Volt/Var control in distribution networks considering distributed generators. Appl Energ 2010; 87: 1919-1928.

[8] Azimi R, Esmaeili S. Multiobjective daily Volt/Var control in distribution systems with distributed generation using binary ant colony optimization. Turk J Elec Eng & Comp Sci 2013; 21: 613-629.

[9] Oshiro M, Tanaka K, Uehara A, Senjyu T, Miyazato Y, Yona A, Funabashi T. Optimal voltage control in distribution systems with coordination of distribution installations. Int J Elec Power 2010; 32: 1125-1134.

[10] Kim YJ, Ahn SJ, Hwang PI, Pyo GC, Moon SI. Coordinated control of a DG and voltage control devices using a dynamic programming algorithm. IEEE T Power Syst 2013; 28: 42-51.

[11] Mohammadi S, Mozafari B, Soleymani S. Optimal operation management of microgrids using the point estimate method and firefly algorithm while considering uncertainty. Turk J Elec Eng & Comp Sci 2014; 22: 735-753.

[12] Liang RH, Chen YK, Chen YT. Volt/Var control in a distribution system by a fuzzy optimization approach. Int J Elec Power 2011; 33: 278-287.

[13] Malekpour AR, Tabatabaei S, Niknam T. Probabilistic approach to multi-objective Volt/Var control of distribution system considering hybrid fuel cell and wind energy sources using improved shuffled frog leaping algorithm. Renew Energ 2012; 39: 228-240.

[14] Homaee O, Zakariazadeh A, Jadid S. Real-time voltage control algorithm with switched capacitors in smart distribution system in presence of renewable generations. Int J Elec Power 2014; 54: 187-197.

[15] Zakariazadeh A, Homaee O, Jadid S, Siano P. A new approach for real time voltage control using demand response in an automated distribution system. Appl Energ 2014; 117: 157-166.

[16] Zhong J, Bhattacharya K. Toward a competitive market for reactive power. IEEE T Power Syst 2002; 17: 1206-1215.

[17] Gomes MH, Saraiva JT. Allocation of reactive power support, active loss balancing and demand interruption ancillary services in MicroGrids. Electr Pow Syst Res 2010; 80: 1267-1276.

[18] Özgönenel O, Thomas DWP. Short-term wind speed estimation based on weather data. Turk J Elec Eng & Comp Sci 2012; 20: 335-346.

[19] Ullah NR, Bhattacharya K, Thiringer T. Wind farms as reactive power ancillary service providers—technical and economic issues. IEEE T Energy Conver 2009; 24: 661-672.

[20] Zare M, Niknam T. A new multi-objective for environmental and economic management of Volt/Var control considering renewable energy resources. Energy 2013; 55: 236-252.

[21] Slimani L, Bouktir T. Economic power dispatch of power systems with pollution control using artificial bee colony optimization. Turk J Elec Eng & Comp Sci 2013; 21: 1515-1527.

[22] Wong S, Bhattacharya K, Fuller J. Long-term effects of feed-in tariffs and carbon taxes on distribution system. IEEE T Power Deliver 2010; 25: 1241-1253.

[23] Lamont JW, Fu J. Cost analysis of reactive power support. IEEE T Power Syst 1999; 14: 890-898.

[24] Ghadikolaei HM, Tajik E, Aghaei J, Charwand M. Integrated day-ahead and hour-ahead operation model of discos in retail electricity markets considering DGs and CO2 emission penalty cost. Appl Energ 2012; 95: 174-185.